LOSSES IN HYBRID AND ACTIVE MAGNETIC BEARINGS APPLIED TO LONG TERM FLYWHEEL ENERGY STORAGE

L. BAKAY*, M. DUBOIS*, P. VIAROUGE*, J. RUEL †

* Electrical Engineering Department, LEEPCI, Laval University, QC G1V 0A6
† Mechanical Engineering Department, Design Bureau, Laval University, QC G1V 0A6
Quebec-City, CANADA
e-mail: loicq-serge.bakay.1@ulaval.ca

Keywords: PM-Biased magnetic bearing, Active magnetic bearing, Long Term Flywheel Energy Storage, losses, Flywheel discharge time.

Abstract

In this work, Radial Active Magnetic Bearings (RAMB) and PM-biased Hybrid Radial Magnetic Bearings (HRMB) were designed and optimized in the case of the Flywheel Long Term Energy Storage (LTFES). Taking into account the amplitude of external disturbance as well as unbalance force as load capacity, the effect of losses (non including losses in the power electronic) on the both RAMB and PM-biased HRMB was studied. Flywheel discharge times have been computed and drawn for a flywheel rotating at a nominal speed of 9000 rpm and self-discharging down to half-speed (4500 rpm). The evolution of this time duration versus mass of bearings is shown for different values of unbalance forces for these two magnetic bearing configurations.

1 Introduction

Flywheel Energy Storage (FES) draws increasing attention thanks to its high number of charge and discharge cycles compared to batteries. The application of the FES as a means of storing energy for a long term period (up to 24 hours) requires a long self-discharge period. The flywheel discharge time will depend on the overall FES losses including bearings, motor/generator drive and friction aerodynamic losses. The latter can be reduced by using a vacuum housing. In order to eliminate friction losses of the mechanical bearings, magnetic bearings can be used, exhibiting absence of contact between the rotating and non-rotating parts of the flywheel. To insure the flywheel stabilization, radial and axial magnetic bearings are often used. In this paper, we will focus on the radial magnetic bearings which can be Permanent Magnet (PM)-Biased or totally active. [6], [2],[4] have widely discussed about Radial Active Magnetic Bearings (RAMB) principles with their control and the authors [1] have studied the effect of the amplitude of unbalance on the RAMB loss while [7], [3] presented the concepts of PM-biased Hybrid Radial Magnetic Bearings (HRMB). In this work, these two models are designed and optimized in the case of the Flywheel Long Term Energy Storage (LTFES). Figure 1 presents the Flywheel assembly.

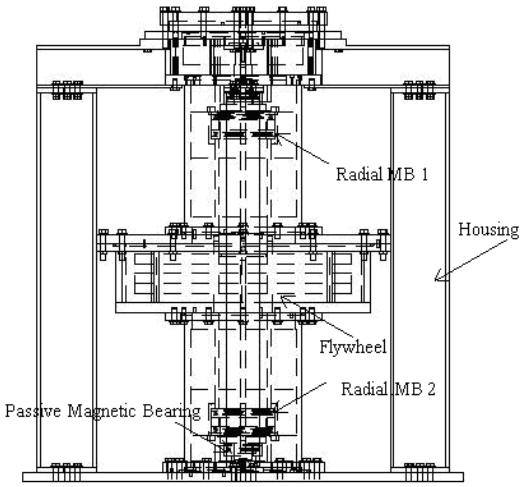

Fig.1: Flywheel assembly

2 Flywheel Mass Unbalance

A rotating mass is subject to external forces, which may be constant, either synchronous or non-synchronous with the rotor angular velocity or they can be less predictable — earth-quake for instance. To simplify this work, we restricted the effect of external disturbance to a constant unbalance force only. Whatever balancing quality is specified for a rotating element, some residual unbalance will be present at start and further unbalance may develop in service. This unbalance gives rise to synchronous forces that may provide very important excitation of rotor-bearing system [3]. These radial forces determine the force requirement of radial AMB. Therefore, AMB electromechanical devices have to take into account the flux flowing in the AMB core due to the response of the amplifier, with respect to the disturbance.

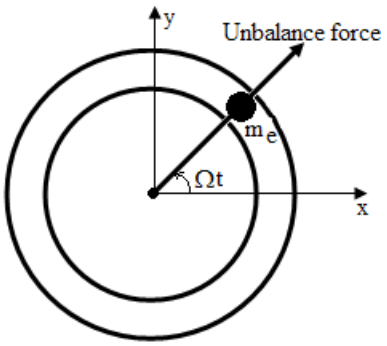

Fig. 2: Unbalance mass principle (Flywheel top view)

Figure 2 shows the principle of unbalance force generation, wherein the rotor is considered as perfectly symmetrical but having an additional mass m_e (kg) at a radius of ε(m) with an angle Ωt, where Ω (rad/s) is the rotational angular speed of the rotor. The radial force is projected on the x-y axes as defined by [4].

$$F_x = m_e \varepsilon \Omega^2 \cdot Cos(\Omega t) \qquad F_y = m_e \varepsilon \Omega^2 \cdot Sin(\Omega t) \qquad (1)$$

The amplitude of these forces is proportional to the square of rotational speed. Generally, m_e and ε are unknown and depend on acceptable eccentricity of the center of gravity specific to the application. Denoting ε_{CG} the eccentricity of the center of gravity of the <u>whole</u> rotor of mass m, the unbalance force is then $F = m\varepsilon_{CG}\Omega^2$, where $m\varepsilon_{CG}$ corresponds to the rotor unbalance U(kg-m). Thus the unbalance force may be simplified as the product of unbalance U and the square of the rotation speed Ω.

$$F_{\max} = U \cdot \Omega^2 \qquad U = \frac{G}{\Omega} \cdot m \qquad (2)$$

The G parameter is the quality grade of the balancing. Typical values of the balancing grade G are given in [5] for several applications. For a flywheel, the typical value for G is 6.3 mm/s. It must be mentioned that although G is generally expressed in mm/s, for equations (2) to be consistent, calculations must be performed with G expressed in m/s. From equation (2), it can also be observed that the balancing quality grade G depends on the product of unbalance and rotational speed. From (2), we can infer the maximum force F_{rmax} which acts on each radial AMB and which, with a security factor, will fix the design of the AMB.

$$F_{r\max} = \frac{U \cdot \Omega^2}{2} \qquad (3)$$

Factor 1/2 is introduced because we are in presence of two radial magnetic bearings: One above the flywheel (MB1) and one below the flywheel (MB2) as depicted in figure 1. Since unbalance is assumed as sinusoidal, the current density (current) in the expressions (4) and (7) set in the coils will be assumed to be sinusoidal as well.

3 Radial Magnetic Bearings forces

3.1 Radial Active Magnetic Bearings

In the AMB literature, we commonly find radial AMBs with three, four, six or eight poles and the choice depends on either the requirements or the complexity of the application.

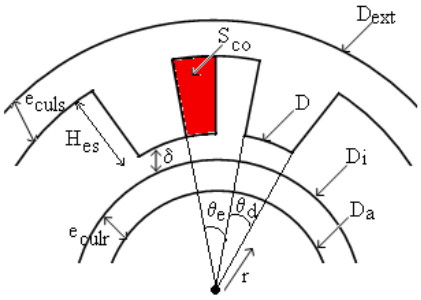

Fig. 3: Analysis model of Radial AMB

Figure 3 shows the cross-section of an eight-pole RAMB. The maximum electromagnetic force of each RAMB is nonlinear and proportional to the square of current density as given in equation (3). Factor k takes into account the dimensions of the RAMB [4]. In order to take into account the effective section of winding, a winding filling factor α is introduced.

$$F_m(t) = J^2(t) \cdot S_{co}^2 \cdot \mu_0 \theta_d L \cdot \frac{d}{d\delta}\left(\ln\left(\frac{D}{D_i}\right)^{-1} \right) = k \cdot J^2(t) \qquad (4)$$

$$k \approx \alpha \cdot \frac{{S_{co}}^2 \cdot \mu_0 \cdot L \cdot (D/2) \cdot \theta_d}{\delta^2} Cos\left(\pi/8\right) \qquad (5)$$

For the purpose of control, either J or i which are respectively the current density and the current is often decomposed into two parts: J_0 or I_0 ensuring the stiffness of the rotor and Δj or Δi allowing compensation of change of the disturbance force.

Hence, the maximum radial force $\hat{F}_m$ of each AMB becomes:

$$\hat{F}_m = k \cdot \left(J_0 + \Delta\hat{J} \right)^2 \qquad (6)$$

Taking into account that, in the case of a displacement Δx of the rotor the current must be decreased in a coil and increased in the radially facing one by an amount Δj (or Δi), the resulting force of each axis of RAMB which will keep the rotor centered is given by expression (7)

$$\begin{aligned} F_r(t) &= F_{m1}(t) - F_{m2}(t) \\ &= k \cdot \left[\left(J_0 + \Delta j(t) \right)^2 - \left(J_0 - \Delta j(t) \right)^2 \right] \\ &= 4 \cdot k \cdot J_0 \cdot \Delta j(t) \end{aligned} \qquad (7)$$

3.2 PM-Biased Hybrid Radial Magnetic Bearings

Even though HRMB can be used in a 3-pole configuration, 4-pole PM-biased configuration (fig. 4) is used in this application for better simplicity.

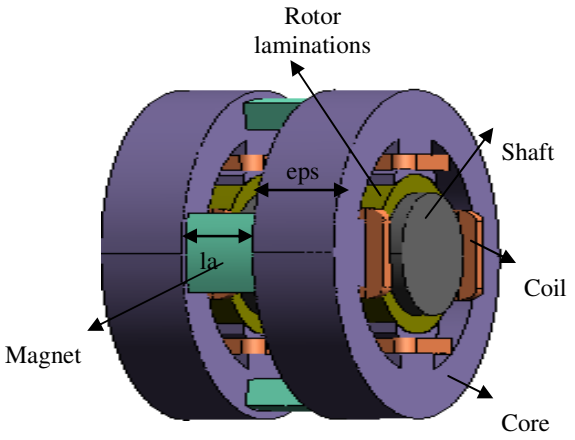

Fig. 4: RHMB geometry

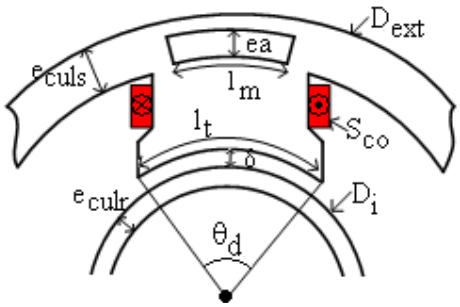

Fig. 5: RHMB analysis model

Commonly, RHMB is constituted by front and back iron as shown in figure 4. These two parts of the stator are separated by four permanent magnets. A coil is wound around each pole except when back iron is passive *i.e.* without any coils. Two coils radially facing are series connected. The flux due to the coils flows from a pole into the radial opposite pole through the stator and rotor yokes and air-gap. This flux flows in the radial plan of laminations while the flux due to permanent magnets flows in the axial plan of laminations.

The flux densities due to the permanent magnet and to the current in the air-gap are respectively given by expressions (8) and (9).

$$B = B_r \frac{l_{PM}}{\frac{S_t}{S_{PM}} + 2\cdot\delta} \tag{8}$$

$$B_\delta = \mu_0 \frac{N\cdot\Delta i_p}{\delta} \tag{9}$$

The electromagnetic force obtained on a part of the stator is given in (10)

$$F_{tot} = \frac{1}{2\mu_0} S_t \left[\left(B + B_\delta\right)^2 - \left(B - B_\delta\right)^2 \right] \tag{10}$$

Taking into account that there are two parts of stator, the total radial electromagnetic force F_{rad} acting on the rotor is twice bigger than F_{tot} as expressed in (11).

$$F_{rad}(t) = B_r \frac{4\cdot S_t \cdot S_{co} \cdot S_{PM} \cdot l_{PM}}{\delta\cdot(S_t \cdot l_{PM} + 2\cdot\delta\cdot S_{PM})} \cdot \Delta j_p(t) \tag{11}$$

The electromagnetic force in PM-biased HRMB is naturally linear with the current as expressed in equation (11); the bearing geometric parameters such as S_t (tooth total flux cross section), S_{co} (copper section), S_{PM} (permanent magnet flux cross section), l_{PM} (PM axial length), δ (air-gap) and the PM residual flux density B_r are constants.

In this case, the stiffness of the rotor comes from the bias flux generated by permanent magnets.

$$F_{rad}(t) = k' \cdot \Delta j_p(t) \tag{12}$$

$$k' = B_r \frac{4\cdot S_t \cdot S_{co} \cdot S_{PM} \cdot l_{PM}}{\delta\cdot(S_t \cdot l_{PM} + 2\cdot\delta\cdot S_{PM})} \tag{13}$$

$$\begin{cases} S_t = l_t \cdot eps \\ S_{PM} = l_m \cdot ea \end{cases} \tag{14}$$

3.3 Magnetic bearings specifications

The radial force expressed for each radial bearing configuration must be at the least equal to F_{rmax}. This force has been set as constraint of optimization for each bearing configuration.

$$4\cdot k \cdot J_0 \cdot \Delta j = k' \cdot \Delta j_p = \frac{U\cdot\Omega^2}{2} \tag{15}$$

The evolution of the current density as a function of the rotational speed is given for the both bearings in equation (16)

$$\Delta j(\Omega) = \Delta j(\Omega_{\max}) \cdot \left(\frac{\Omega}{\Omega_{\max}} \right)^2 \tag{16}$$

Because the amplitude of the unbalance force is proportional to the square of the rotational angular speed of the rotor, the

current densities increase or decrease according to the equation (16).

4 Losses and discharge time computation

In this section 3, radial magnetic bearings force was computed for each bearing configuration for the purpose of setting the latter as a constraint in the optimization, which has to be greater than the amplitude of the unbalance chosen as the load capacity.

Radial Bearings maximum O.D	Dext	270 mm
Number of poles (RAMB)	8	∅
Number of poles (RHMB)	4	∅
Coils turn (for each electromagnet)	N	100
Air gap	δ	1 mm
Flywheel shaft diameter	Da	100 mm
MB maximum axial length	L	150 mm
Flywheel rotor mass	m	200 kg
Maximum rotational speed	Ωmax	9000 rpm
Minimum rotational speed	Ωmin	4500 rpm
Quality grade of the balancing	G	6.3 mm/s

Table 1: Input data of radial bearings

Table 1 indicates all the constraints of magnetic bearings have to fulfil. Maximum outer diameter D_{ext} and maximum axial length L of each magnetic bearings configuration have been fixed from the flywheel housing size. These parameters and others are presented in Table 1.
In this section, losses and flywheel discharge time are studied by taking into account the presence of an unbalance (presented in section 2) on the rotor. Losses have been computed and their evolutions against rotational speed are shown below.

4.1 Losses computation

In the case of Long Term Flywheel Energy Storage, loss of the overall system is one of critical parameters and need to be minimized.. This study is restricted to radial magnetic bearing design (non including amplifiers). Figure 6 presents a flywheel active power distribution.

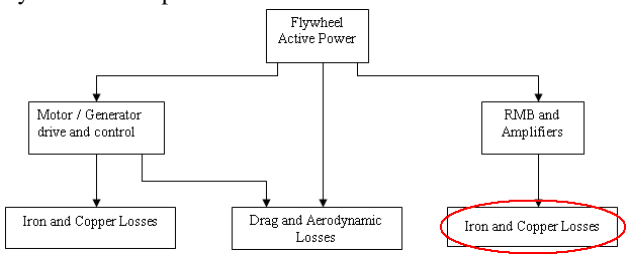

Fig. 6: Flywheel Losses flowchart

Losses in RAMB are often greater than those of PM-biased HRMBs when the latter are well designed. Neglecting iron losses in stator is justified in the case of an ordinary Flywheel Energy Storage; in the Long Term Flywheel Energy storage iron losses in stator are not neglected because flywheel supplies itself. Any sources of loss, which heat-up the rotor and slow down the latter, have to be taken into account.

A) Copper Losses

In both bearing configurations, copper Losses due to the current flowing in the coils to oppose the unbalance force are located in stator only. Assuming the currents in the coils as sinusoidal, copper losses can be written as follows:

For the RAMB:

$$P_{coRAMB} = \rho_{co} \cdot V_{coRAMB} \cdot \left(J_0 + \frac{\Delta \hat{J}}{\sqrt{2}} \right)^2 \qquad (17)$$

For the RHMB:

$$P_{coHRMB} = \rho_{co} \cdot V_{coHRMB} \cdot \frac{\Delta \hat{J}_p^2}{2} \qquad (18)$$

Because of the current density J_0, constant copper losses appear even in the absence of any disturbance in the case of the RAMB. The RAMB coil volume is greater than in the PM-HRMB.

B) Iron Losses

Usually, iron losses are divided into two components eddy currents losses P_{eddy} and hysteresis losses P_{hyst} as shown in equation (19); those are located in the stator and in the rotor for both configurations. To reduce eddy currents losses, laminated materials are used. In absence of any disturbance, only the bias current flows in the coils of the RAMB, which does not generate iron losses in stator. However, in presence of unbalance force, iron losses occur in the stator of the RAMB.

In this study hysteresis and eddy current losses are considered.

$$P_{iron} = P_{hyst} + P_{eddy} \qquad (19)$$

Or,

$$p_{iron} = k_h B^n f + k_{ed} B^2 f^2 \qquad (20)$$

The coefficients k_h, k_{ed} and n depend on the thickness and the conductivity of the laminated material used.

The variation of flux density B in the air-gap due to the bias flux generated by permanent magnets — HRMB — or by the bias current — RAMB — generates iron losses in the rotor according to relationship (20). An optimization was made for the purpose of minimizing the mass of each bearing configurations and then, the design obtained was reported in

Finite Element Model software (MagNet) in order to determine iron losses.
Using the expression (20) for iron losses computation in the rotor, f is twice bigger than the mechanical frequency because two flux density periods are contained in a geometric period of rotor as discussed in [4].

4.2 Flywheel discharge time computation

For computing discharge time, magnetic bearings constraints given in table 1 were used. Some curves such as Loss Torque LT (figure 7) and Losses (figure 8) versus rotor angular speed Ω, which are inferred from a same magnetic bearing design are essential for the flywheel discharge time computation. Total losses associated to the bearings are the sum of both the magnetic losses and copper losses. At Ω = 0, unbalance force and magnetic losses are zero according to (2) and (20). In this case, the bearings do not need any compensation current and therefore, losses are essentially due to the copper losses (due to I_0 in the case of RAMB). In Long Term Flywheel Energy Storage, this occurs either at start-up. As flywheel supplies itself via motor/generator drive, at start-up both bearing configurations need an external source of energy to keep the flywheel centered.

The linear regression form of loss torque is expressed as:

$$T_L = A \cdot \Omega + B \tag{21}$$

A is the loss torque slope and B the value of the torque at Ω = 0. During the self discharge period, from the dynamic equation, the torque of both the flywheel and radial bearings can be written as (22), where J_f is the flywheel moment of inertia.

$$J_f \frac{d\Omega}{dt} + T_L = 0 \tag{22}$$

Assuming that $\Omega = \Omega_{max}$ à t = 0, expression for the flywheel speed (22) is the solution of equations (21) and (22).

$$\begin{cases} \Omega(t) = \left(\Omega(0) + \dfrac{B}{A} \right) \cdot e^{\frac{A}{J_f} t} - \dfrac{B}{A} \\ \Omega(0) = \Omega_{\max} \end{cases} \tag{23}$$

The discharge time t_f is the time required for the flywheel, to see its speed decay from the maximum speed Ω_{max} to the minimum speed Ω_{min} taking into account the losses of the bearings only. Expression of that time is

$$t_f = \ln\left(\frac{\Omega_{\min} + \dfrac{B}{A}}{\Omega_{\max} + \dfrac{B}{A}} \right) \cdot \frac{J_f}{A} \tag{24}$$

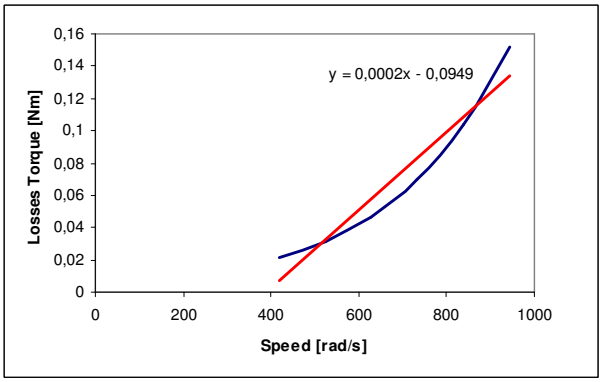

Fig. 7: PM-HRMB Losses torque evolution

The maximum and minimum speeds of the flywheel are respectively 9000 RPM and 4500 RPM

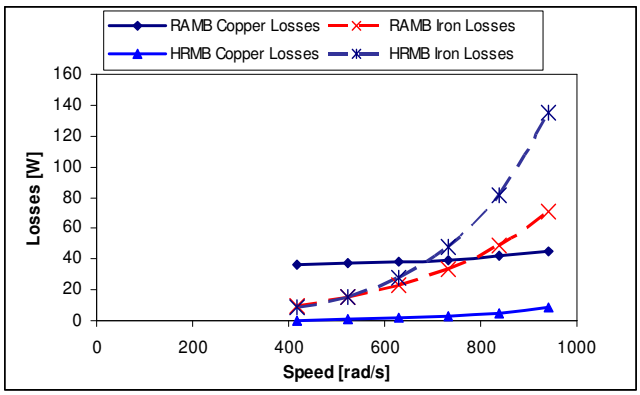

Fig. 8: Magnetic bearings Losses

Figure 8 shows the evolution of losses of magnetic bearings in function of the rotational speed. As expected, when the speed increases total losses increase because iron Losses and Copper Losses increase according to (15), (16), (17) and (19). Copper losses in RAMB are higher than in the PM-HRMB. At low speeds Iron losses in the both RAMB and HRMB are same but become higher in HRMB above 525 rad/s.

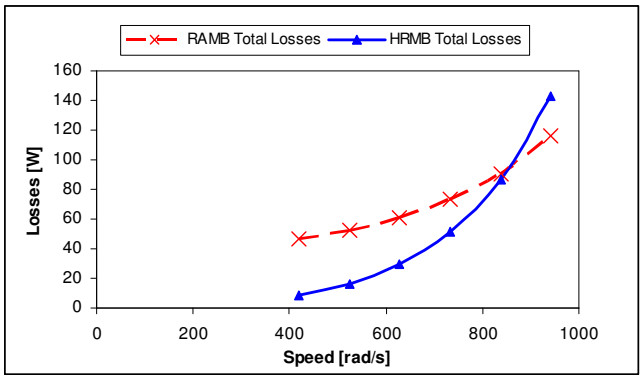

Fig. 9: Total Losses of Magnetic bearings

In figure 9 we remark that total losses in RAMB are higher than those in PM-HRMB under a certain speed; this effect inverts above 840 rad/s, then total losses in PM-HRMB become higher. Therefore, the energy extracted from the flywheel is higher for HRMBs above 840 rad/s than in RAMBs.

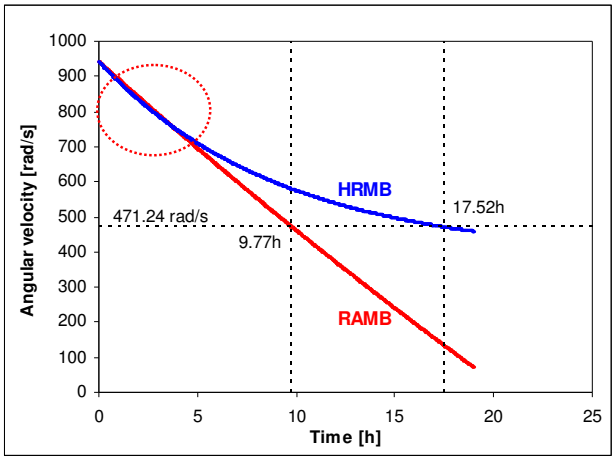

Fig. 10: Flywheel discharge time

Figure 10 presents the flywheel discharge time evolution in function of angular velocity. Flywheel takes 9.77h to pass from 942 rad/s to 471rad/s when RAMB are used while it takes 17.5h when HRMB are used.

4 Conclusion

To quantify losses induced by radial suspension in Long Term Flywheel Energy Storage, radial magnetic bearing designs were presented. The effect of rotational speed on the losses of two configurations of bearings was especially shown and the flywheel discharge time in function of the speed was drawn. To overcome unbalance force, currents are injected in the coils. Hence losses increase, and the flywheel discharge time decreases. It emerged that, HRMB total losses are higher than those of RAMB above a certain speed. It recommended operating flywheel at low speed in the case of a Long Term Flywheel Energy Storage.

For radial magnetic bearings of 270mm of outer diameter and 150mm of length, the discharge times reported to slow down from 9000 rpm to 4500 rpm are respectively 9.75h (which means important losses) for RAMB and 17.5h for HRMB.

Reference

[1] L.Bakay et al. "Losses in an Optimized 8-pole Radial AMB for Long Term Flywheel Energy Storage", *12th ICEMS*. Nov. 16-18, 2009, Tokyo, Japan

[2] A.Chiba, T. Fukao, O. Ichikawa, M. Oshima, M. Takemoto and D.G Dorrell "Magnetic bearings and bearingless Drives" *Newnes – Elvesier publications* - 2005, ISBN 0 7506 5727 8.

[3] A.C.Lee, F.Z.Hsiao, D.Ko "Analysis and testing of magnetic bearing with permanent magnets for bias", *JSME International Journal*, Vol.37, No.4, 1994.

[4] F. Matsumura and K. Hatake, "Relation between magnetic pole arrangement and magnetic loss in magnetic bearing," in *Proc. 3rd Int. Symposium Magnetic Bearings*, Alexandria, VA, July 1992, pp. 274–283.

[5] A.V. Ruddy "Rotor dynamics of turbo-machinery", *The Glacier Metal Co.Ltd*, Industrial Lubrication and Tribology, April 1984

[6] G.Schweitzer, H. Bleuler and A. Traxler, "Active Magnetic Bearings" *Vdf Hochschlverlag AG* an der ETH Zürich, 1994.

[7] Christopher K. Sortore et al. "Permanent Magnet Biased Magnetic Bearings –Design, Construction and Testing", *2nd International Symposium on Magnetic Bearings*. July 12-14, 1990, Tokyo, Japan